Graphene Oxides

DOI: 10.1002/anie.201310908

Ozonated Graphene Oxide Film as a Proton-Exchange Membrane**

Wei Gao, Gang Wu, Michael T. Janicke, David A. Cullen, Rangachary Mukundan, Jon K. Baldwin, Eric L. Brosha, Charudatta Galande, Pulickel M. Ajayan, Karren L. More, Andrew M. Dattelbaum, and Piotr Zelenay**

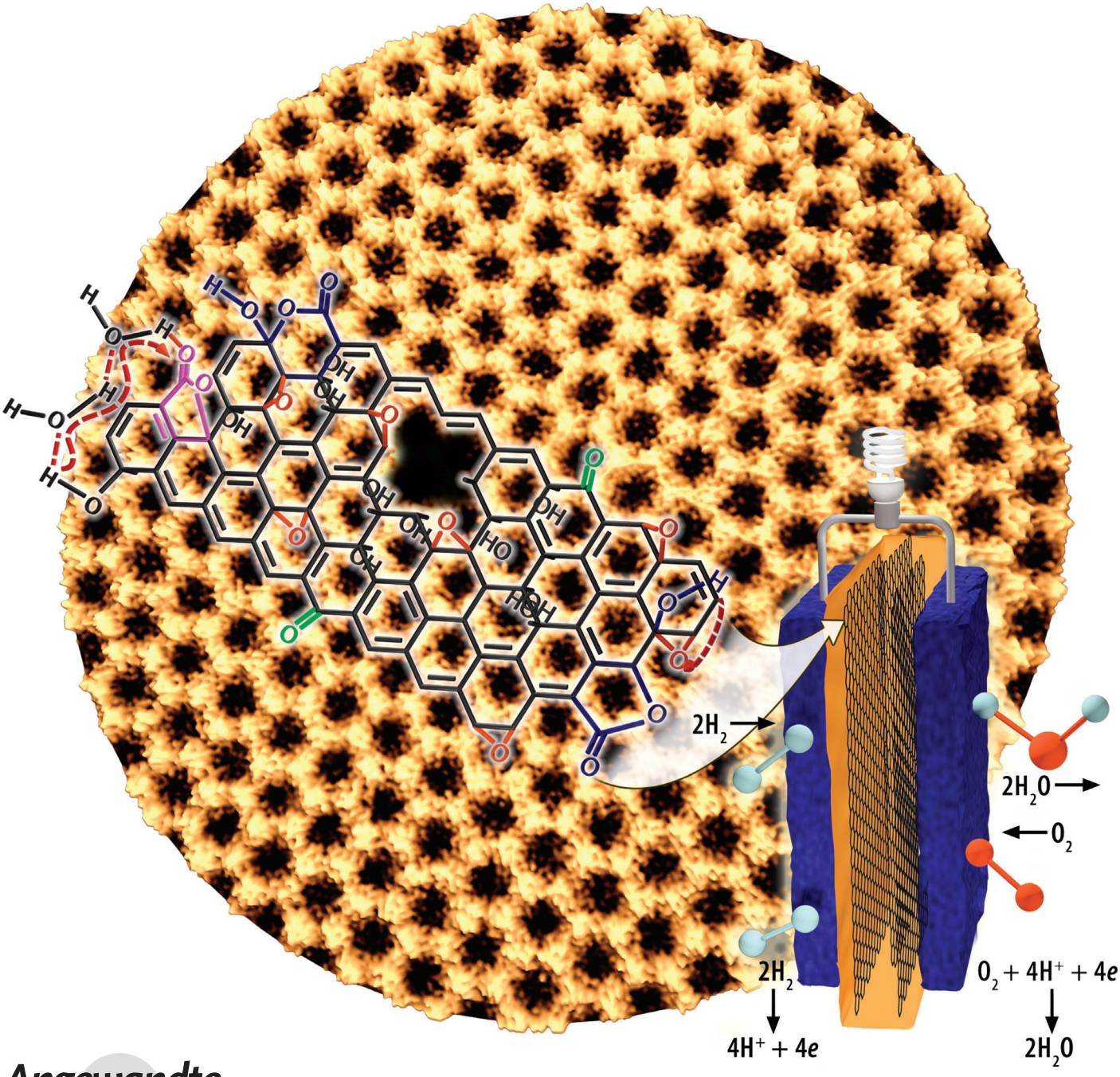

Abstract: *Graphene oxide (GO) contains several chemical functional groups that are attached to the graphite basal plane and can be manipulated to tailor GO for specific applications. It is now revealed that the reaction of GO with ozone results in a high level of oxidation, which leads to significantly improved ionic (protonic) conductivity of the GO. Freestanding ozonated GO films were synthesized and used as efficient polymer electrolyte fuel cell membranes. The increase in protonic conductivity of the ozonated GO originates from enhanced proton hopping, which is due to the higher content of oxygenated functional groups in the basal planes and edges of ozonated GO as well as the morphology changes in GO that are caused by ozonation. The results of this study demonstrate that the modification of dispersed GO presents a powerful opportunity for optimizing a nanoscale material for proton-exchange membranes.*

Soon after the discovery of graphene,[1] graphene oxide (GO) started to attract considerable interest from researchers all over the world as a potential precursor to graphene and because of its unique electronic and optical properties.[2] The GO surface is functionalized with various oxygen-containing groups, predominantly hydroxy and epoxy moieties, on both its basal planes and edges.[3] Recently, it was reported that GO forms freestanding films with an inherent ionic conductivity that can be utilized in monolithic supercapacitors.[4] A Grotthuss mechanism, in other words, proton hopping through a hydrogen-bonding network, was suggested as a possible way for the movement of protons in GO, although this issue remains the subject of intense debate.[4,5] Furthermore, the properties of GO can be chemically modified for particular applications much more easily than those of graphene owing to the pre-existence of functional groups on the GO surface.[6]

Herein, we show that the chemical modification of GO by ozone to form ozonated GO (OGO) results in a material with a higher percentage of oxygenated functional groups. Filtration of OGO was used to make freestanding OGO films. We determined the proton-conducting properties of freestanding GO and OGO films in a fuel cell and found the OGO films to have an approximately 50% higher protonic conductivity at 100% relative humidity (RH). This increase may be attributed to an increase in the number of proton-hopping sites that results from a greater number of oxygen-containing functional groups in OGO than in GO, as well as from the addition of pinholes and smaller sheet sizes in OGO after ozonation, which was observed by scanning transmission electron microscopy (STEM). Such modified GO films may be of significant interest to polymer electrolyte fuel cells (PEFCs), which rely on proton-conducting membranes between the anode and the cathode.

GO is known to be metastable at room temperature, losing epoxy groups and gaining hydroxy groups within a relaxation half-lifetime of about one month.[7] Herein, we describe that the treatment of GO with ozone (O_3) led to an increase in the hydroxy, lactol, ester, and ketone content of GO, as observed by solid-state ^{13}C magic-angle-spinning (MAS) nuclear magnetic resonance (NMR) spectroscopy (Figure 1; see also the Supporting Information, Figure S1; for the sake of comparison, the spectra in Figure 1a were scaled to the height of the tallest peak, C–O–C.) Deconvolution and integration of the peak areas that are assigned to different functional groups allowed us to determine the content of sp^2-hybridized carbon atoms as 17.5 and 31.5 at% in OGO and GO, respectively. This implies that 82.5 and 68.5 at% of the carbon atoms are oxygenated in OGO and GO, respectively. These results demonstrate that ozonation is an effective technique for increasing the degree of oxidation in GO. Ozone has previously been reported to facilitate the attachment of oxygen atoms to sp^2-hybridized carbon atoms in single-walled carbon nanotubes, which enhanced the fluorescence of individual nanotubes.[8] The inset in Figure 1a shows the color change for a GO/H_2O dispersion before and after ozonation, which can be explained by structural changes and a corresponding band-gap opening in GO upon ozonation. The detailed reaction mechanism is illustrated in Figure 1b and discussed in the Supporting Information.

Structural changes between GO and OGO can be further studied by FTIR and UV/Vis absorption spectroscopy, X-ray photoelectron spectroscopy (XPS), X-ray diffraction (XRD),

[*] Dr. W. Gao, Dr. G. Wu, Dr. R. Mukundan, J. K. Baldwin, Dr. E. L. Brosha, Dr. A. M. Dattelbaum, Dr. P. Zelenay
Materials Physics and Applications Division
Los Alamos National Laboratory
Los Alamos, NM 87545 (USA)
E-mail: amdattel@lanl.gov
zelenay@lanl.gov

Dr. M. T. Janicke
Chemistry Division, Los Alamos National Laboratory
Los Alamos, NM 87545 (USA)

Dr. D. A. Cullen, Dr. K. L. More
Materials Science and Technology Division
Center for Nanophase Materials Sciences
Oak Ridge National Laboratory
Oak Ridge, TN 37831-6064 (USA)

C. Galande, Prof. P. M. Ajayan
Department of Mechanical Engineering and Material Science
Rice University
Houston, TX 77251 (USA)

[**] Support from the Office of Energy Efficiency and Renewable Energy of the U.S. Department of Energy (DOE) through the Fuel Cell Technologies Office and from Los Alamos National Laboratory through the Laboratory Directed Research and Development (LDRD) program and a Director's Postdoctoral Fellowship for W.G. is gratefully acknowledged. This work was done in part at the Center for Integrated Nanotechnologies, an Office of Science User Facility operated for the U.S. DOE Office of Science by Los Alamos National Laboratory and Sandia National Laboratories. This research was supported in part by Oak Ridge National Laboratory's Center for Nanophase Materials Sciences (CNMS), which is sponsored by the Scientific User Facilities Division, Office of Basic Energy Sciences, US DOE.

Supporting information for this article is available on the WWW under http://dx.doi.org/10.1002/anie.201310908.

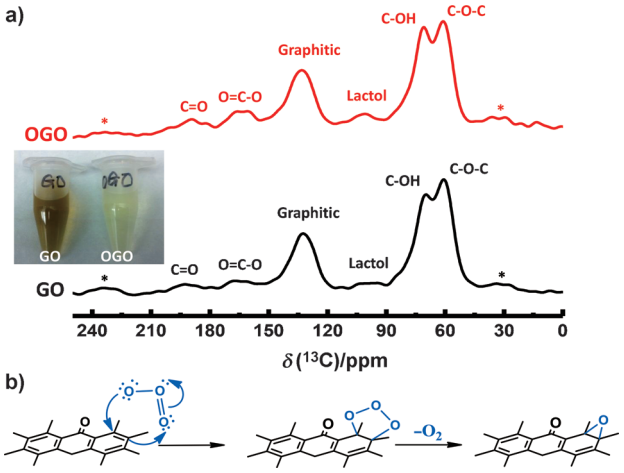

Figure 1. Ozonation of GO. a) Direct ^{13}C pulse MAS NMR spectra of GO and OGO samples. For the sake of comparison, the spectra were scaled to the height of the tallest peak (C–O–C). The star (*) denotes spinning sidebands on both sides. Inset: Images of GO and OGO dispersions in deionized water. b) The reaction between O_3 molecules and a basal plane of GO.

and thermogravimetric analysis (TGA; Figure S2 and S3). The structural and morphological changes after ozonation were also characterized by annular dark-field (ADF)-STEM. Single-layer GO and OGO samples were frequently observed (Figure 2a,b). Pinholes were found in both the GO and OGO samples. According to ADF-STEM image analysis, the average pinhole diameter for both GO and OGO was close

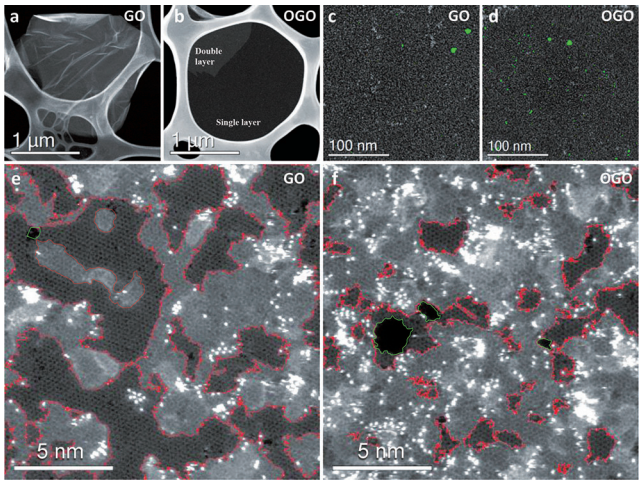

Figure 2. ADF-STEM images of GO and OGO samples. a,b) Low-magnification images of GO and OGO films. c,d) Images of pinholes in GO (c) and OGO (d); pinholes are shown in green to enhance visibility. e,f) Atomically resolved images of GO (e) and OGO (f) that show the difference in surface coverage of disordered regions that are associated with oxygen functionalization. The borders between graphene regions (darker contrast) and disordered regions are outlined in red, whereas pinholes are outlined in green. The individual bright spots in the ADF images were identified to be silicon, a contaminant that is commonly found in graphene and graphene oxide. Because of their much larger atomic number, the Si atoms dominate the contrast in the image, but EELS and XPS both found that the total Si content was only 1–2 at%.

to 2.5 nm, whereas the ozonation treatment led to a dramatic increase in the number density of pinholes, from 325 ± 55 pinholes μm^{-2} in GO to 1135 ± 225 pinholes μm^{-2} in OGO (pinholes are indicated in green for GO and OGO in Figure 2c and 2d, respectively).

ADF-STEM images also revealed that the individual GO and OGO sheets consist of small areas of defective graphene regions that are intermixed with a network of what appears to be a more disordered material (outlined in red in Figure 2e and 2f for GO and OGO, respectively). Our data is consistent with previous TEM studies on GO that indicated that most of the surface oxygen-based functional groups are associated with disordered regions.[9] A comparison of the ADF-STEM images that were acquired for GO and OGO shows a clear difference in the extent of surface coverage of the disordered regions. For GO, the disordered regions accounted for approximately 65% of the total surface area, whereas the extent of surface coverage on OGO increased to 85%, suggesting an increase in oxygen functionalization that was caused by the ozonation process. These percentages for the disordered areas in GO and OGO are consistent with the amounts of oxygenated carbon atoms in GO and OGO that were determined by solid-state MAS NMR spectroscopy (Figure 1a).

Anisotropic ionic conductivity has previously been observed for GO at high humidity.[4,5] The in-plane ionic conductivity in GO is approximately two orders of magnitude higher than that in the perpendicular direction; however, it is currently difficult to access the bulk in-plane conduction in a practical way. Therefore, the GO and OGO sheets were aligned perpendicular to the proton-conduction pathways. Possible ionic pathways through the bulk films are depicted in Figure 3a; movement may occur along the edges and pinholes of the 2D sheets. As a result, the smaller sheet size and higher pinhole density in OGO, which was observed by ADF-STEM, are expected to improve its proton conduction relative to that of GO films. The transverse protonic conductivity of both GO and OGO increases with increasing humidity (Figure 3b). At 100% relative humidity (RH), the conductivity of the OGO film is 50% higher than that of the GO film. The results from electrochemical impedance spectroscopy (EIS) and a comparison of the GO and OGO films are given in Figure S4.

To ensure that the ionic conductivity is due to the transfer of protons rather than electrons or other ions, the voltage drop across an OGO film was measured as a function of the difference in hydrogen (H_2) partial pressure on both sides of the film (see the Supporting Information for experimental details).

In such an experiment, the potential of the Pt electrodes is controlled by the fast and fully reversible electrochemical reaction of hydrogen oxidation and evolution:

$$H_2 \rightleftharpoons 2H^+ + 2e \qquad (1)$$

The voltage measured across the cell is equal to the difference in the Nernst potentials of the two electrodes (ΔE):

$$\Delta E = t_i \frac{RT}{2F} \ln\left(\frac{P(H_2)_1}{P(H_2)_2}\right) \qquad (2)$$

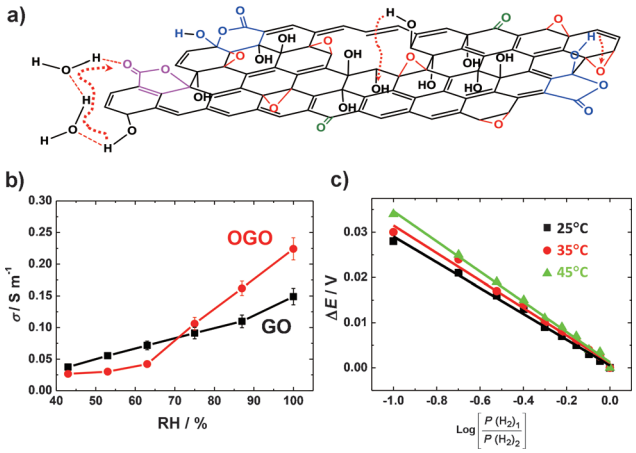

Figure 3. Transverse protonic conductivity of GO and OGO films. a) Proton hopping in an OGO flake across the edges and pinholes by hydrogen bonding with water molecules (lower left corner). Functional groups are differentiated by color. Proton-hopping routes are highlighted with red dotted arrows. b) Dependence of the conductivity on relative humidity (RH), as determined by EIS. c) Cell voltage as a function of the difference in H_2 partial pressure on both sides of an OGO film.

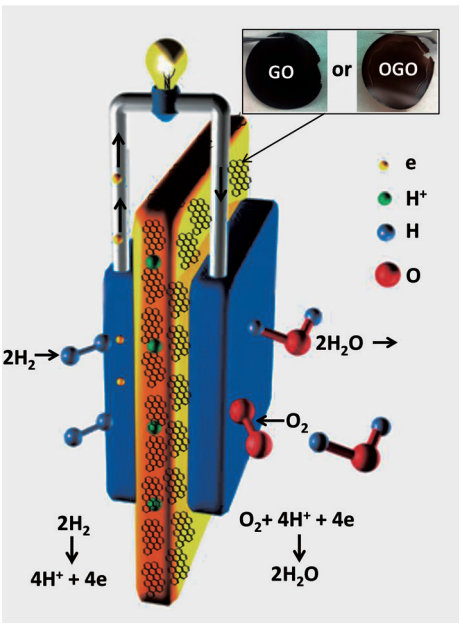

Figure 4. A GO/OGO membrane incorporated into a polymer electrolyte fuel cell. Inset: photographs of freestanding GO and OGO membranes that were made from the same batch of GO.

Here, t_i is the transference number (the total current that is carried by a certain charge carrier, a proton in this case), $p(H_2)_1$ and $p(H_2)_2$ are the partial pressures of hydrogen at electrode 1 and electrode 2, respectively, R is the universal gas constant (8.314 $J K^{-1} mol^{-1}$), T is the absolute temperature (K), 2 is the number of electrons transferred in reaction (1), and F is the Faraday constant (96.485 $C mol^{-1}$). Experiments were conducted at 25 °C, 35 °C, and 45 °C.

The slopes of the ΔE versus log $\Delta p(H_2)$ lines that were obtained at the relatively low temperatures of 25 °C and 35 °C, 28.5 mV dec^{-1} and 30.4 mV dec^{-1}, respectively, are very close to the theoretical values of 29.5 mV dec^{-1} (25 °C) and 30.5 mV dec^{-1} (35 °C; Figure 3c). At a higher temperature of 45 °C, the measured slope of 33.4 mV dec^{-1} shows a slightly larger deviation from the theoretical value of 31.5 mV dec^{-1}, which may be due to a mixed potential that is caused by the leakage of a small amount of O_2.[10] In agreement with this interpretation, a similar deviation was also observed with Nafion membrane at these temperatures (Figure S5). Assuming that the proton transference number of Nafion is 1.0 under these conditions, the OGO film has proton transference numbers of 0.99, 0.97, and 1.0 at 25 °C, 35 °C, and 45 °C, respectively. These experiments offer direct evidence for *proton* conduction in OGO films. Furthermore, EIS measurements of an OGO film under a pure H_2 atmosphere gave minimum interfacial resistance and mass transfer resistance (see Figure S6), which corroborates the hypothesis that proton conduction occurs.

Given the protonic conductivity of bulk GO films described above, we performed a series of hydrogen/air fuel cell tests to assess the feasibility of using a freestanding OGO film as a proton-conducting membrane. A schematic illustration of an OGO film that is incorporated in a fuel cell is shown in Figure 4. Compared to conventional fuel cell structures, the major distinction is the use of a carbon-based, non-polymeric membrane for protonic conduction. The inset in Figure 4 shows photographs of the GO and OGO membranes used. As discussed above, OGO is more oxidized than GO and has a larger band gap; this results in the OGO membrane being of a lighter brown color than the GO film.

Our experiments can also be contrasted with other reports that describe the use of GO or functionalized GO as an additive to Nafion composites, with the resulting properties dominated by the Nafion polymer.[11] The tests were carried out at a moderate temperature of 35 °C and at 100 % RH. Freestanding GO and OGO films, both 22 μm in thickness, were prepared from the same batch of dispersed GO. The voltage–current polarization plots are shown in Figure 5a. The corresponding high-frequency resistance (HFR) data are given in Figure 5b. At a current density of 0.25 A cm^{-2}, the OGO/GO ratio of protonic conductivity is approximately 1.7. This value, which was obtained at a single frequency of 3.3 kHz, is somewhat higher than the OGO/GO conductivity ratio that is determined from the full-frequency range, and thus likely to be more accurate (for impedance spectra, see Figure 3b). Better ionic conductivity appears to be the main reason for the superior performance, which has improved by a factor of approximately two, of the OGO film compared to the GO film (Figure 5a).

Long-term fuel cell tests were also performed for freestanding GO and OGO films at 35 °C (Figure 5c). The OGO membrane maintained higher performance than the GO membrane throughout the 100-hour tests. Although the OGO stability is not sufficient for practical applications at present, we were able to improve it by using a sandwich configuration. The sandwich consisted of two Nafion 212 layers on both sides of a GO/OGO film that prevented direct exposure to

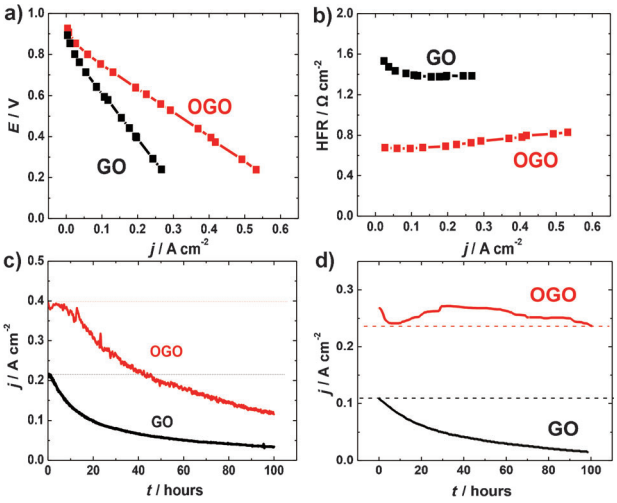

Figure 5. Hydrogen/air fuel cell performance with freestanding GO and OGO films as proton-exchange membranes. a) *j*–*V* plots. b) Ionic resistance at a single frequency of 3.3 kHz as a function of current density. c) Long-term stability tests of pristine GO/OGO membranes in fuel cells at 35 °C. d) Long-term stability tests of GO/OGO sandwiched between Nafion membranes in fuel cells at 35 °C.

hydrogen and possible reduction of the oxygen functional groups. The Nafion–OGO–Nafion sandwich operated for 100 h at 35 °C with little evidence of performance loss (Figure 5 d). Further improvements in fuel-cell performance may also be expected by additional functionalization and re-alignment of GO flakes in the membrane. We have only used the transverse proton conduction in our experiments thus far (Figure S7). Utilizing the higher in-plane conductivity[4,5] by aligning OGO flakes parallel to the proton-hopping pathway is the subject of ongoing experiments.

Finally, some highly graphitic and anisotropic carbon materials, in particular single-walled nanotubes, potentially represent alternative materials for the carbon-based, proton-conducting membranes that were obtained by the ozonation method described.

Herein, we have shown that dispersed GO may be chemically modified to improve the properties of a bulk film that is made entirely of functionalized GO nanomaterial. We have verified that the conduction in OGO and GO films is due to protons. We successfully implemented both films in hydrogen/air fuel cells, a first demonstration of freestanding proton-conducting membranes that are derived directly from oxidized graphene in fuel cells of any kind.

The enhancement in protonic conductivity of OGO versus GO likely originates from changes in chemical structure and morphology that are caused by the ozonation process. A higher content of oxygenated functional groups on the edges and basal planes of graphene is expected to offer more hopping sites (conduction channels) for protons. The morphological changes, in particular a decrease in the flake size and an increase in pinhole density, can also afford additional pathways for proton hopping or diffusion through the bulk films, which leads to higher protonic conductivity. Considering the anisotropic nature of proton conduction in GO and OGO[4,5] and its potential for further optimization, GO derivatives could become a carbon-based, non-polymeric alternative to Nafion for hydrogen fuel cell, supercapacitor,[4] catalysis,[12] and sensing[13] applications.

Experimental Section

GO was prepared according to a modified version of Hummers method.[14] A GO/H_2O dispersion (5 mg mL^{-1}) was ozonated by bubbling O_3 gas through the dispersion, which was placed in a water bath and subjected to mild sonication. The resulting OGO dispersion was vacuum-filtered through a cellulose membrane (0.22 μm; Millipore) to obtain a freestanding OGO film. Fuel cell tests were carried out in a single cell with serpentine flow channels (Fuel Cell Technologies, Inc.). Solid-state NMR, XPS, XRD, FTIR, TGA, STEM, and EIS were used for sample characterization. Please see the Supporting Information for experimental details.

Received: December 17, 2013
Published online: February 14, 2014

Keywords: fuel cells · graphene oxide · ionic conductivity · ozonation · proton-exchange membrane

[1] K. S. Novoselov, A. K. Geim, S. V. Morozov, D. Jiang, Y. Zhang, S. V. Dubonos, I. V. Grigorieva, A. A. Firsov, *Science* **2004**, *306*, 666 – 669.

[2] a) D. A. Dikin, S. Stankovich, E. J. Zimney, R. D. Piner, G. H. B. Dommett, G. Evmenenko, S. T. Nguyen, R. S. Ruoff, *Nature* **2007**, *448*, 457 – 460; b) R. Ruoff, *Nat. Nanotechnol.* **2008**, *3*, 10 – 11; c) K. P. Loh, Q. Bao, G. Eda, M. Chhowalla, *Nat. Chem.* **2010**, *2*, 1015 – 1024; d) D. Li, M. B. Muller, S. Gilje, R. B. Kaner, G. G. Wallace, *Nat. Nanotechnol.* **2008**, *3*, 101 – 105.

[3] a) W. Gao, L. B. Alemany, L. Ci, P. M. Ajayan, *Nat. Chem.* **2009**, *1*, 403 – 408; b) W. Cai, R. D. Piner, F. J. Stadermann, S. Park, M. A. Shaibat, Y. Ishii, D. Yang, A. Velamakanni, S. J. An, M. Stoller, J. An, D. Chen, R. S. Ruoff, *Science* **2008**, *321*, 1815 – 1817; c) A. Kolmakov, D. A. Dikin, L. J. Cote, J. Huang, M. K. Abyaneh, M. Amati, L. Gregoratti, S. Gunther, M. Kiskinova, *Nat. Nanotechnol.* **2011**, *6*, 651 – 657; d) S.-S. Li, K.-H. Tu, C.-C. Lin, C.-W. Chen, M. Chhowalla, *ACS Nano* **2010**, *4*, 3169 – 3174.

[4] W. Gao, N. Singh, L. Song, Z. Liu, A. L. M. Reddy, L. Ci, R. Vajtai, Q. Zhang, B. Wei, P. M. Ajayan, *Nat. Nanotechnol.* **2011**, *6*, 496 – 500.

[5] M. R. Karim, K. Hatakeyama, T. Matsui, H. Takehira, T. Taniguchi, M. Koinuma, Y. Matsumoto, T. Akutagawa, T. Nakamura, S.-i. Noro, T. Yamada, H. Kitagawa, S. Hayami, *J. Am. Chem. Soc.* **2013**, *135*, 8097 – 8100.

[6] a) Y. Zhu, S. Murali, W. Cai, X. Li, J. W. Suk, J. R. Potts, R. S. Ruoff, *Adv. Mater.* **2010**, *22*, 3906 – 3924; b) D. R. Dreyer, S. Park, C. W. Bielawski, R. S. Ruoff, *Chem. Soc. Rev.* **2010**, *39*, 228 – 240.

[7] S. Kim, S. Zhou, Y. Hu, M. Acik, Y. J. Chabal, C. Berger, W. de Heer, A. Bongiorno, E. Riedo, *Nat. Mater.* **2012**, *11*, 544 – 549.

[8] a) S. Ghosh, S. M. Bachilo, R. A. Simonette, K. M. Beckingham, R. B. Weisman, *Science* **2010**, *330*, 1656 – 1659; b) J. D. Fortner, D.-I. Kim, A. M. Boyd, J. C. Falkner, S. Moran, V. L. Colvin, J. B. Hughes, J.-H. Kim, *Environ. Sci. Technol.* **2007**, *41*, 7497 – 7502.

[9] a) K. Erickson, R. Erni, Z. Lee, N. Alem, W. Gannett, A. Zettl, *Adv. Mater.* **2010**, *22*, 4467 – 4472; b) D. Pacilé, J. Meyer, A. Fraile Rodriguez, M. Papagno, C. Gomez-Navarro, R. Sundaram, M. Burghard, K. Kern, C. Carbone, U. Kaiser, *Carbon* **2011**, *49*, 966 – 972.

[10] R. Bouchet, E. Siebert, G. Vitter, *J. Electrochem. Soc.* **2000**, *147*, 3125 – 3130.

[11] a) A. Enotiadis, K. Angjeli, N. Baldino, I. Nicotera, D. Gournis, *Small* **2012**, *8*, 3338 – 3349; b) Y.-C. Cao, C. Xu, X. Wu, X. Wang, L. Xing, K. Scott, *J. Power Sources* **2011**, *196*, 8377 – 8382; c) B. G. Choi, J. Hong, Y. C. Park, D. H. Jung, W. H. Hong, P. T. Hammond, H. Park, *ACS Nano* **2011**, *5*, 5167 – 5174.
[12] a) G. Gelbard, *Ind. Eng. Chem. Res.* **2005**, *44*, 8468 – 8498; b) L. A. Paquette, D. Crich, P. L. Fuchs, G. A. Molander, *Encyclopedia of Reagents for Organic Synthesis*, *Vol. 14*, *2nd ed.*, Wiley, Hoboken, **2009**.
[13] C. Heitner-Wirguin, *J. Membr. Sci.* **1996**, *120*, 1 – 33.
[14] S. Gilje, S. Han, M. Wang, K. L. Wang, R. B. Kaner, *Nano Lett.* **2007**, *7*, 3394 – 3398.

